03

Dielectric spectroscopy of doped sillenites crystals

© A.V. Ilinskiy[1], R. Castro[2], L.A. Nabiullina[3], E.B. Shadrin[1]

[1] Ioffe Institute,
St. Petersburg, Russia
[2] Herzen State Pedagogical University of Russia,
St. Petersburg, Russia
[2] Fire and Rescue College and Rescue Training Center,
St. Petersburg, Russia

E-mail: shadr.solid@mail.ioffe.ru

Received May 29, 2024
Revised May 29, 2024
Accepted June 18, 2024

In the frequency range $10^{-2}-10^{8}$ Hz at a temperature of 300 K, the dielectric spectra of undoped and doped Ni, Mn, Co, Cu, Fe, Mo high-resistivity ($\rho > 10^{10}$ Ohm · m) sillenite crystals ($Bi_{12}SiO_{20}$) were studied. It is shown that the detected features of the spectra are due to the response of an array of free electrons, the dark concentration of which is determined by the presence of donor or acceptor impurities. The results of calculating dielectric spectra within the framework of the Debye theory, as well as within the framework of a complicated theory using the function $G(\tau)$ of the distribution of numbers of relaxers over their relaxation times, are presented. The relaxation times of the response to the action of a probing electric field are estimated and it is shown that they are determined by the Maxwellian relaxation times for electrons. The parameters of the function $G(\tau)$ are determined. It is shown that a significant variation in relaxation times for different impurities is due, in addition to differences in electron concentrations, to the dependence of the electron drift mobility on the parameters of traps in the presence of which charge transfer occurs. Key words: dielectric spectra, dielectric loss tangent, Debye distribution, charge transfer, sillenite crystals, Maxwellian relaxation time.

Keywords: dielectric spectra, dielectric loss tangent, Debye distribution, charge transfer, sillenite crystals, Maxwellian relaxation time.

DOI: 10.61011/PSS.2024.08.59049.141

1. Introduction

Sillenite crystals are oxides of type $Bi_{12}MO_{20}$ (M = Ge, Si, Ti) and relate to spatial group I23. Important features of sillenites are: low dark electrical conductivity, high photosensitivity in the visible spectral range and the absence of an inversion center, which leads to the presence of bright photorefractive effects in these crystals. Such effects determine the possibility of optical recording and processing of information in devices based on sillenite crystals [1,2].

As the sillenite crystals are widely used as controllable optical transparencies, and in applied laser technologies when creating adaptive holographic interferometers, the physical parameters of which are determined by the counter interaction of electromagnetic waves in the visible range. The main region of application of this type of interferometers relates to the procedure of contactless control of deformations and flaw detection of metal structures in the production of power units for bridge construction, as well as in large-scale mechanical engineering [3]. Besides, sillenites are used in holographic cameras as dynamic carrier of optical recording [4]. Such camera operates in pulse mode and is used to analyze vibrations of designed facilities. Besides the production tasks the same camera is used for space studies (when constructing space telescopes). Photorefractive crystals, being adaptive reusable information carriers, by several times increase, due to presence of holographic camera, the range of measurement of external influence parameters in comparison with other optical interference systems. Besides, BSO crystals are indispensable in holographic devices of multiple diagnostic instruments to monitor yielding phenomena on board of space objects of type of international space station [5,6].

It should be emphasized that in sillenite crystals almost all photorefractive effects are due to the process of charge transfer inside the crystal either under action of concentration gradient of free carriers of current (electrons), formed by heterogeneous illumination, or as result of application of an external electric field. Rather informative methods of study the processes of charge transfer in the sillenite crystals are methods used linear Pockels electro-optical effect [7]. Besides, effective method for studying processes of charge transfer in crystals is method of dielectric spectroscopy [8–10]. Its essence is measurement of frequency dependence of complex current at $I^*(\omega)$ application to sample of external reference alternating voltage $U_0(\omega)$. Recently, the method of dielectric spectroscopy has gained popularity due to the development and creation of industrial dielectric spectrometers with high sensitivity and equipped with computers with modern software packages for experimental data processing.

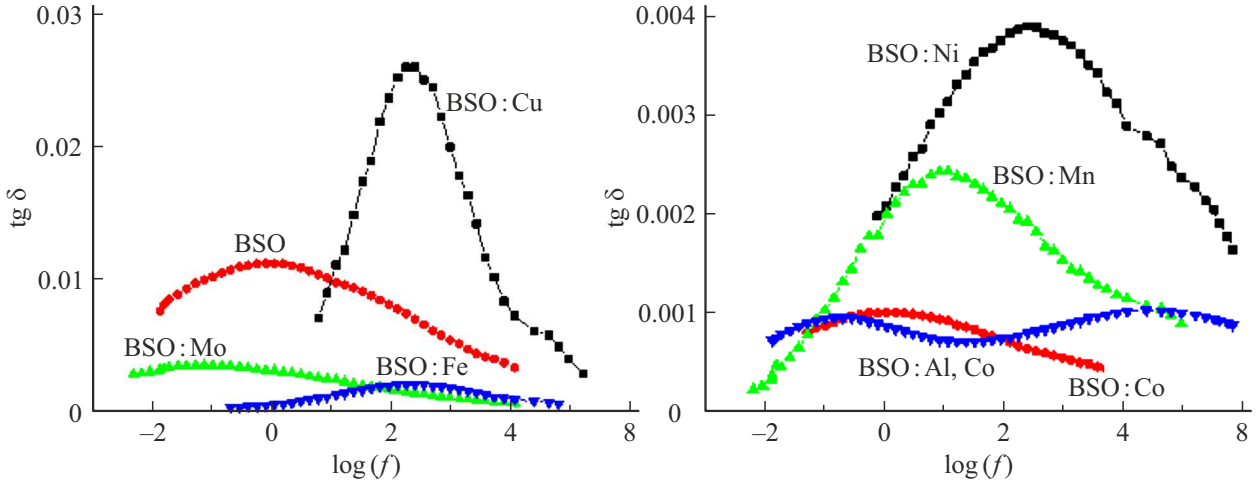

Figure 1. Frequency dependencies $\mathrm{tg}\,\delta(f)$ for samples of stilletes crystals doped with impurity of copper, molybdenum, iron, nickel, magnesium, cobalt and two impurities of aluminium and cobalt at room temperature.

The present paper task is study by methods of optical spectroscopy of the processes of charge transfer by dark current carriers both in undoped, and in doped crystals $Bi_{12}SiO_{20}$ (BSO). The fact is that crystals doping with various chemical elements not only changes the concentration of the main charge carriers, but also varies ratio of concentrations of deep and shallow traps [11], at which „sticking“ of current carriers occurs during their drift. This means that doping affects also the drift mobility of the charge carriers. These circumstances lead to a change in the characteristics of the process of shielding the external electric field, which, as this paper shows, is clearly visible in dielectric spectra (DS).

2. Experimental procedure

Samples studied in this paper were thin (about 1 mm) transparent crystals $Bi_{12}SiO_{20}$ of light-yellow color, synthesized by Czochralski method. Crystals were doped by the following impurities in process of synthesis: Co, Cu, Al, Fe, Mo, Mn, Ni.

looseness-1 For studied crystals at room temperature ($T = 293$ K) in spectrometer „Concept-81“ (Novocontrol Technologies GmbH) in wide range if frequencies ($f = 10^{-2}$–10^{6} Hz) DS of satellites samples were obtained upon absence of light illumination. Namely, frequency dependences of components of complex electric impedance of studied samples were obtained. Prior to measurements the crystals were in dark for 1 h.

Exactly during studies the real and imaginary parts of the complex impedance of the cell with the sample under study were registered.

$$Z^*(\omega) = \frac{U_0}{I^*(\omega)}.$$

Based on the obtained information the frequency spectra of complex dielectric permittivity were determined

$$\varepsilon^* = \varepsilon' - i\varepsilon'' = \frac{-i}{\omega Z^*(\omega)}\frac{1}{C_0},$$

where $C_0 = \frac{\varepsilon_0 S}{d}$ — electric capacity of cell without sample.

The obtained in such way spectra were converted in spectra of dielectric loss angle tangent $\mathrm{tg}\,\delta(\omega) = \varepsilon''(\omega)/\varepsilon'(\omega)$, and by exclusion of frequency ω as parameter they were rearranged as functions $\varepsilon''(\varepsilon')$, determined as Cole–Cole diagram. Such functions without any additional information about sample, make the important features registered by DS more apparent.

3. Experimental results

Figure 1 presents frequency dependences of dielectric loss angle tangent $\mathrm{tg}\,\delta(f)$ of undoped and doped by one or simultaneously two impurities of samples BSO, obtained at room temperature. Practically in all these dependences there is one maximum located in region of frequencies $f = 10^{-2}$–10^{6} Hz. Absolute value of dielectric loss angle tangent is rather low: $\mathrm{tg}\,\delta(f) \ll 1$, indicating significant exceedance by displacement currents of the drift currents of free charge carriers, which definitely confirms the fact of the presence of very low dark conductivity of the crystals under study. Besides, It is fundamentally important that the frequency positions of the DS maxima for different doping impurities differ from maximum position for undoped crystal BSO. So, for impurities Ni, Cu, Mn and Fe they are located in region of higher frequencies, for other impurities (Mo, Co) — in region of lower frequencies in relation to undoped BSO. It is interesting that with simultaneous doping with two impurities (Al and Co) in the DS, two weak maxima are observed on the frequency dependence

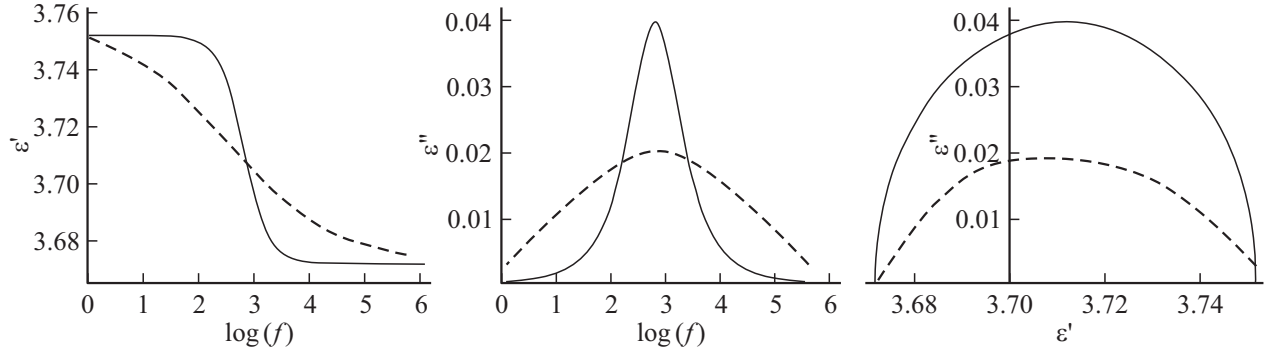

Figure 2. Frequency dependences $\varepsilon'(f)$, $\varepsilon''(f)$ obtained at room temperature and Cole–Cole diagram for samples of satellites crystals doped with impurity of nickel. Dashed curves — measurement results. Solid curves were plotted as per formula (1) and aligned along the axis of abscisses such that Debye frequency $f = 1/(2\pi\tau_D)$ coincides with frequency position fmax of experimentally registered maximum $\varepsilon''(f)$: $\tau_D = 1.6 \cdot 10^{-4}$ s.

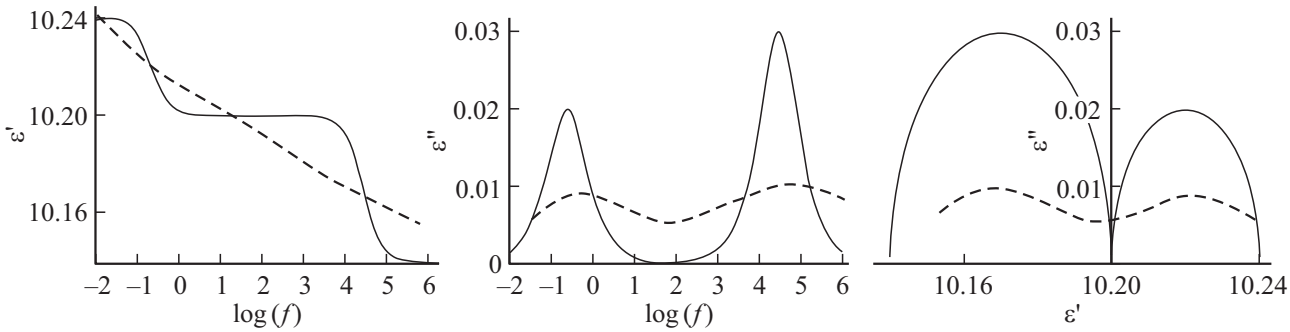

Figure 3. Frequency dependences $\varepsilon'(f)$, $\varepsilon''(f)$ and Cole–Cole diagram for samples of satellites crystals doped by impurity of cobalt and aluminium. Dashed curves — experimental results. Solid curves plotted by formula (2) and aligned in axis of abscisses such that Debye frequencies $f_1 = 1/(2\pi\tau_{D1})$ and $f_2 = 1/(2\pi\tau_{D2})$ coincide with frequency positions $f_{\max 1} = 10^5$ Hz and $f_{\max 2} = 0.3$ Hz of experimentally registered maxima $\varepsilon''(f)$.

$\operatorname{tg}\delta(f) \approx 0.001$, at that these features are rather wide, i.e. cover rather elongated spectral range: $10^{-2} < f < 10^8$ Hz.

Figure 2, additionally to functions $\operatorname{tg}\delta(f)$, as additional example by dashed curves present frequency dependences of real $\varepsilon'(f)$ and imaginary $\varepsilon''(f)$ parts of dielectric permittivity, and Cole–Cole diagram $\varepsilon''(\varepsilon')$ for sampled doped by nickel (dashed curves). Here in curve $\varepsilon''(f)$ we observed one maximum, at that its frequency position strictly correlates with frequency position of step in curve $\varepsilon'(f)$. Diagram $\varepsilon''(\varepsilon')$ is significantly distorted semicircle, namely, „height" semicircle ($\varepsilon'' = 0.02$) is significantly smaller then its „radius" ($[\varepsilon'_{(f=0)} - \varepsilon'_{(f=\infty)}]/2 = 0.04$).

DS of sample doped by two types of impurities have more complex view. Figure 3 presents frequency dependences $\varepsilon'(f)$, $\varepsilon''(f)$ and Cole–Cole diagram $\varepsilon''(\varepsilon')$ for sample BSO doped simultaneously by cobalt and aluminium dashed curves). For this sample in spectrum of imaginary part $\varepsilon''(f)$ two wide maxima are clearly observed, at that two wide steps in diagram of real function $\varepsilon'(f)$ „merge" in one gradual descent, whilst in Cole–Cole diagram $\varepsilon''(\varepsilon')$ two highly distorted semicircles are clearly observed. It is well known [12,13] that BSO doping with aluminium results in noticeable enlightenment of the crystal accompanied by color change of crystal from light-yellow to practically transparent state in the visible part of the spectrum with a simultaneous multiple increase (at least by an order of magnitude) in its electrical resistance. This fact correlates with the fact that array of free electrons upon their low concentration can not effectively screen the external sounding electrical field. Namely, experiment gives value $\varepsilon''(f) \approx 0.01$, although heights of both steps of function $\varepsilon'(f)$ are so small that $\operatorname{tg}\delta(f) \approx 0.001$, i.e. in this case $\operatorname{tg}\delta(f) \ll 1$ is actual.

4. Calculation results

The experimental features of DS are qualitatively described by Debye's formula [14,15]:

$$\varepsilon^*\omega = \varepsilon_\infty + \frac{\Delta\varepsilon}{[1 + i\omega\tau_D]}, \qquad (1)$$

where ω — the cyclic frequency, τ_D — relaxation time, i — imaginary unit. $\Delta\varepsilon = \varepsilon'_\infty - \varepsilon'_0$.

Presence of one maximum for the imaginary part of dielectric permittivity $\varepsilon''(f)$, one step[for real part $\varepsilon'(f)$

and single semicircle $\varepsilon''(\varepsilon')$ in Cole–Cole diagram confirms presence of single individual type of relaxers. Note that existence of one individual type of relaxers, as we understand this, indicates the possibility of detection in DS (according to Rayleigh criterion) of one individual maximum of imaginary part of dielectric permittivity $\varepsilon''(f)$.

The spectra $\varepsilon'(\omega) = \varepsilon_\infty + \Delta\varepsilon/[1 + (\omega\tau)^2]$, $\varepsilon'' = \Delta\varepsilon \cdot \tau/[1 + (\omega\tau)^2]$ plotted according to formula (1), as well as diagram $\varepsilon''(\varepsilon')$, are given in logarithmic scale in Figure 2. Parameters of formula (1) are selected such that plotted calculated curves correspond to experiment curves in Figure 2; in particular, Debye frequency $f = 1/(2\pi\tau_D)$ coincides with frequency position $f_{\max} = 10^3$ Hz of maximum $\varepsilon''(f)$. Comparison of graphs shows that Debye theory describes DS shape with quality.

To adequately describe the measurement results presented in Figure 3, expression (1) shall be, according to our opinion, converted into expression (2), which considers superposition of two type of relaxation processes with relaxation time τ_{D1} and τ_{D2} respectively:

$$\varepsilon^*(\omega) = \varepsilon_\infty + \frac{\Delta\varepsilon_1}{[1 + (i\omega\tau_{D1})]} + \frac{\Delta\varepsilon_2}{[1 + (i\omega\tau_{D2})]}. \quad (2)$$

Curves $\varepsilon'(f)$, $\varepsilon''(f)$ and $\varepsilon''(\varepsilon')$, plotted according to expression (2), are given in Figure 3. They also adequately, but only qualitatively, describe the experimental results in Figure 3.

Anyway, upon thorough review of the experimental results in Figure 2 and Figure 3 we can state that maxima and steps in experimental curves are wide by two times then in design curves, and measured CC-diagrams do not have shape of regular semicircles. Namely, „heights" of semicircles of experimental CC-diagrams-is lower then half of their „width".

A more accurate (quantitative) correspondence between the calculation results and the experimental data can be achieved by introducing into consideration of the function $G(\tau)$, having physical meaning of density distribution of relaxers over relaxation times for each individual type of relaxers. In this case, the expression for the frequency dependence of complex dielectric permittivity (equation (1)) is written as

$$\varepsilon^*(\omega) = \varepsilon_\infty + \Delta\varepsilon \int_0^\infty \frac{G(\tau)}{1 + i\omega\tau}\, d\tau. \quad (3)$$

Let's indicate occasionally that expressions (1) and (3) appear to be identical in case when $G(\tau)$ represents δ-function (filtering property of Dirac δ-function [16]).

In our case, when there are DS features by many times exceeding in width the Debye distribution, function $G(\tau)$ is much wider of the typical presentation of δ-function, generally used during analysis of the experimental data. It is even much wider the Debye distribution function. On other hand relatively narrow by frequency contour of function $\varepsilon''(f)$ in Debye expression under integral (3), can, in its turn, play the role of filtering function [17].

The filtering action of Debye function comes down to reproducing the form of the graphical representation of the function $G(\tau)$, at that feature of this presentation is direction of axis of axis of abscisses, reverse in relation to initial direction. Reason of this feature occurrence of filtration process is use of logarithmic scale of function $G(\tau)$ presentation and necessity of transition under integral sign (3) from frequency scale to time scale: $\omega = 1/\tau$, and $\log(\tau) = -\log(\omega)$.

This non-trivial property of the filtration process allows us to apply as function $G(\tau)$ introduced under integral (5) the function of the time dependence of the imaginary part of the dielectric permittivity $\varepsilon''(\tau)$, which is designed based on experimentally obtained function $\varepsilon''(f)$. The design process is extremely simple and comes to replacement of variable f by variable τ ($f = 1/2\pi\tau$).

From a physical point of view, this method is completely justified., as real part of the dielectric permittivity contains, as it is known, information of total electric field formed after the sample exposure to external sounding field, while the imaginary part of the dielectric permittivity contains information on time of response (i. e. on relaxation process) of system under study to effect of sounding electric field.

If experimental features of DS are approximated by formula [18]:

$$\varepsilon^*(\omega) = \varepsilon_\infty + \frac{\Delta\varepsilon}{[1 + (i\omega\tau D)^\alpha]^\beta}, \quad (4)$$

then for function $\varepsilon''(\omega)$, calculating power of a complex number and replacing ω by $1/\tau$, we obtain based on (4) after separation of main branch of multi-valued logarithm the following expression:

$$\varepsilon''(\tau) = (\varepsilon_s - \varepsilon_\infty) r^{-\beta/2} \sin\beta\theta, \quad (5)$$

where

$$r = \left[1 + (\tau_D/\tau)^\alpha \sin\left(\frac{(1-\alpha)\pi}{2}\right)\right]^2 + \left[(\tau_D/\tau)^\alpha \cos\left(\frac{(1-\alpha)\pi}{2}\right)\right]^2,$$

$$\Theta = \operatorname{arctg}\left[\frac{(\tau_D/\tau)^\alpha \cos\left(\frac{(1-\alpha)\pi}{2}\right)}{1 + (\tau_D/\tau)^\alpha \sin\left(\frac{(1-\alpha)\pi}{2}\right)}\right].$$

In Figure 4 as example of function $G(\tau)$ the expression (5) is taken for different values of parameters α and β, and calculation results with this function are given for $\varepsilon''(f)$ according to formula (3). The best matching of calculation according to formula (3) with experimental data requires clarification of parameters α and β of function $\varepsilon''(\tau) = G(\tau)$ in expression (5). Software package of dielectric spectrometer following the set algorithm optimal values of parameters as a result of adjusting the calculation to the experiment (see Table), as well as massive

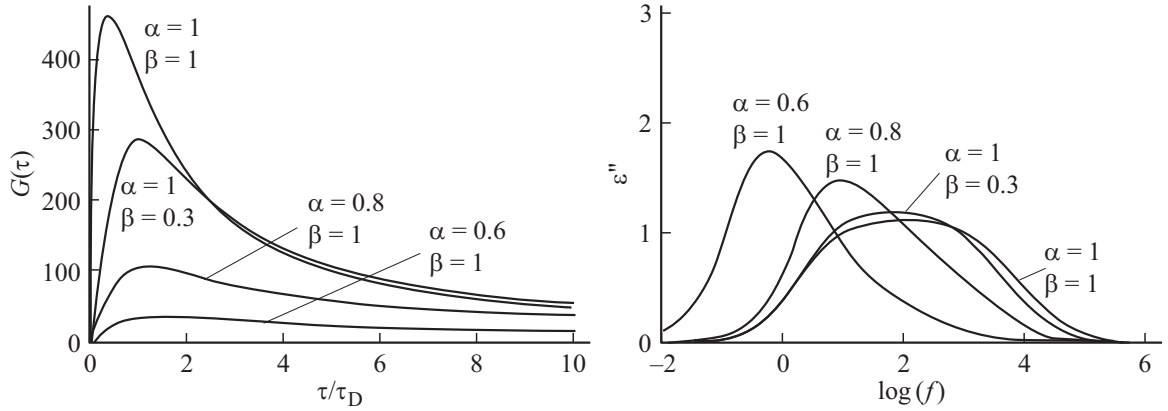

Figure 4. Function $G(\tau)$ — formula (5) with ω replacement by $1/\tau$ and calculation result $\varepsilon''(f)$ as per formula (3) for different values of parameters α and β. $\tau_D = 2.3 \cdot 10^{-4}$ s.

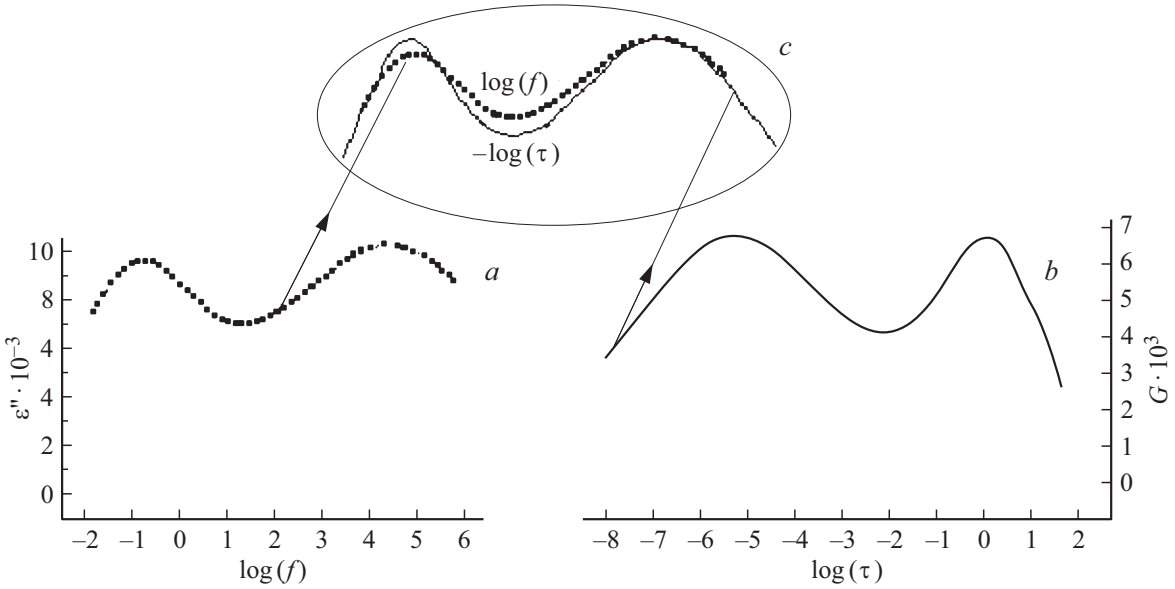

Figure 5. Received at room temperature: frequency dependence $\varepsilon''(f)$ (a) and density distribution function of relaxer over relaxation time $G(\tau)$ (b) for crystals BSO, doped by impurity of cobalt and aluminium. Shape comparison of curves $\varepsilon''(f)$ and $G(\tau)$ (in mirror reflection) shows that maxima $G(\tau)$ are sharper and by 10–12% are narrower then maxima $\varepsilon''(f)$ (insert c).

of data ensuring plotting thew graphs of function $G(\tau)$ both in linear and in logarithmic scales for each option of DS (Figure 1).

Figure 5 as example compares: experimental spectrum $\varepsilon''(f)$ and distribution function $G(\tau)$ for sample BSO : Al, Co, determined for this sample using software of the dielectric spectrometer. Figure shows that function $\varepsilon''(f)$ and mirror rotated function $G(\tau)$ are practically identical within the experimental errors (comp. Figure 5, a and Figure 5, b), but extremely careful comparison of them (inserts Figure 5, c) shows that features in form of maxima of calculated function $G(\tau)$ are by 10–12% narrower then corresponding to them experimental features of DS.

So, when searching structure of function $G(\tau)$ as this function we can take function (4) with selected for experiment parameters α, β and with ω replacement by $1/\tau$. In this case, only for the widest (in comparison with the half-width of the Debye distribution) features of DS, a series of calculations shall be performed using formula (3) with

Value of relaxation parameters provided by computer of dielectric spectrometer during analysis of the experimental dielectric spectra of samples $Bi_{12}SiO_{20}$: Me

Sample	Tau-Max [s]	Alpha	Beta
BSO undoped	$3.96 \cdot 10^{-2}$	0.45	0.43
BSO : Ni	$2.33 \cdot 10^{-4}$	0.29	0.98
BSO : Mn	$9.19 \cdot 10^{-3}$	0.51	0.32
BSO : Co	$1.44 \cdot 10^{-1}$	0.39	0.41
BSO : Cu	$4.28 \cdot 10^{-4}$	0.65	0.81
BSO : Mo	2.16	0.26	0.94
BSO : Fe	$3.81 \cdot 10^{-4}$	0.49	0.98

clarification of the values of the adjustable parameters α and β till good agreement of calculation with measurement results. Function $G(\tau)$, introduced in said way under integral of formula (3) with clarified during integration values of parameters α and β can be assumed as required distribution function of number of relaxer over relaxation times. The function $G(\tau)$ obtained by this method the modern dielectric spectrometers are „positioned" as result of theoretical processing of experimental measurements.

5. Discussion of results

We believe that in our case, the values of DS parameters (the frequency position of the steps $\varepsilon'(f)$, the maxima $\varepsilon''(f)$, the shape and position of the semicircles on CC diagrams) are due to a specific type of relaxers, namely relaxation response of array of free electrons. The characteristic relaxation time in this case is the Maxwellian relaxation times $\tau_{\text{M}} = \varepsilon\varepsilon_0/\sigma$, where σ — the specific electrical conductivity of the crystalline substance.

For undoped BSO in case of free electrons the Maxwellian relaxation time at room temperature is $\tau_{\text{M}} = 4 \cdot 10^{-2}\,\text{s}$ ($f_{\max} = 1/(2\pi\tau_{\text{M}}) = 4\,\text{Hz}$ see. curves in Figure 1), while during samples doping by metals the Maxwellian time change by orders of magnitude.

Determined in such way positions of features of distribution function of relaxers over relaxation times (see Figures 3, 4) on time scale are interpreted by us as follows.

Shift in relation to undoped samples BSO of DS features towards high frequencies during doping by „donor" impurity (Mn, Fe, Ni, Cu, Co) is explained first of all by decrease in electrical resistance of semiconductor, this is possible only due to increase in concentration of free electrons. This means that the shift of the DS features to the high-frequency region is due to a sharp decrease in the Maxwellian relaxation time as a result of doping. On the contrary, shift of features of other spectra towards low frequencies during doping by „acceptor" impurity (Mo) is associated with increase in the resistance of the semiconductor due to decrease in the concentration of free electrons, i. e., a sharp increase in the Maxwellian relaxation time.

But upon simultaneous sample doping by two types of impurities (Co and Al) two DS features are observed (Figure 3), one of them is shifted towards high frequencies, and second one — towards low frequencies. As conductivity of sample at room temperature has only one (fixed) value, then explanation of these two features presence, shifted to opposite sides, is more complex then above mentioned.

First of all we say that formula $\tau_{\text{M}} = \varepsilon\varepsilon_o/\sigma$ is presented in general form, and its appearance shall not be assumed as a ratio of fixed values constant over time τ_{M} and σ. Conductivity of substance is: $\sigma = en\mu$, where e — charge of electron, n and μ — their concentration and drift mobility respectively. In our case there is dependence of conductivity on time: $\sigma(t)$ and, hence, $\tau_M(t)$ are also time functions. Actually, charge transfer in high-resistance sillenite crystals is performed by free electrons upon presence of deep and shallow traps, as a result quasi-free electrons for some time „stick" in these traps. Due to traps presence the drift mobility of electrons decreases, and electrons can be divided into „fast" and „slow". So, conductivity can be presented as $\sigma = e\mu_{\text{fast}}n_{\text{fast}} + e\mu_{\text{slow}}n_{\text{slow}}$. At low times (high frequencies) the array of „fast" electrons shields the external electric field, but incompletely, if, in spite of high mobility μ_{fast}, the concentration of fast electrons is low: See high-frequency step $\Delta\varepsilon_1' = 0.06$ in Figure 3. At large times „slow" electrons continue process of charge transfer and field shielding till displacement from sample of its major portion (but incomplete displacement): step $\Delta\varepsilon_2' = 0.04$ although small, but, however, it is clearly present in Figure 3.

Other possibility to interpret two DS features of crystals BSO, doped by Co and Al, is inclusion in discussion of ambipolar conductance. In other words, the role of fast charge carries is played, for example, by electrons, and role of slow one is played by holes [19].

Actually, probably, both cases are possible. Namely, there are two types of electrons and one type of holes, and the curvature in the K-space of the valence band, as calculations show, is significantly less than the curvature of the conduction band. I.e. holes have at least by five times larger effective mass than electrons, i. e. are obviously „slow". Calculations of paper [19] and results of paper [20] show that effective masses of both types of electrons in crystals BSO are close to each other, i. e. both are „fast", even though one of them belog G-point of Brillouin zone, being „straight". And other are in minimum in N-point of Brillouin zone, being „unstraight".

So, in our case the Maxwellian time has two values, which are widely spaced in their magnitudes. This clearly shows that the dielectric spectroscopy method allows us to separate not only „fonor" and „acceptor" impurities, but also „fast" and „slow" electrons upon presence of several types of traps occurred during simultaneous crystal doping by several types of impurities. Noticeable distribution width $G(\tau)$ of the relaxers in time, that differs from the distribution provided by δ-function, states, by our opinion, about variations of crystal conductivity, which occurs first of all due to noticeable variations of mobility of free carriers, but not variations of their concentration.

6. Conclusion

So, due to very high sensitivity of devices used for study we are able to study DS of high-resistance crystals $Bi_{12}SiO_{20}$ with their rather low dark conductivity ($\sigma < 10^{-10}\,\text{Sim/m}$), at that even in cases when during shielding of the external sounding electric field the difference $\Delta\varepsilon = \varepsilon_\infty - \varepsilon_0$ is rather low: $\Delta\varepsilon = \varepsilon_\infty - \varepsilon_0 < 0.05$ (Figure 3). The same is applied to the dielectric loss angle tangent: $\text{tg}\,\delta < 0.001$ (Figure 1). DS calculation provided in the paper both within framework of Debye theory, and within framework of more complicated theory comprising analytical expression

of density distribution function of relaxers over their times, will show that DS features of both undoped and doped crystals BSO are due to presence of free electrons in low, but different concentration for undoped and doped crystals. For all studied samples numerical values of relaxation time are determined of samples response to effect of the external electrical field. Physical mechanism is suggested for interrelation of frequency position of DS features and nature of samples doping by impurities of different metals. It is shown that the relaxation times of electrical response are determined by Maxwellian relaxation time $\tau_M = \varepsilon\varepsilon_o/\sigma$, at that these times have noticeable variation of the crystals conductivity $\sigma = e\mu n$. The obtained results provide the conclusion that such variation is determined by significant dependence of drift mobility μ of electrons on trap parameters (concentration, sections of catching and activation energies E_i), in the presence of which the charge transfer occurs. I.e. variation is determined by that these parameters significantly differ for traps of various types.

Funding

The study was performed under the State Assignment with financial support of Ministry of Education of Russia (Project No. VRFY-2023-0005).

Conflict of interest

The authors declare that they have no conflict of interest.

References

[1] P. Lemaire, M. Georges. In: Photorefractive Materials and Their Applications 3. Springer Series in Optical Sciences **115**. Springer. N.Y. 223 (2007).
[2] A.A. Kamshilin, R.V. Romashko, Y.N. Kulchin. J. Appl. Phys. **105**, *3*, 1381 (2009).
[3] A.A. Kolegov, L.A. Kabanova. FTT: Sb. mater. XII Ros. nauch. stud. konf. Tomsk, 163 (2010). (in Russian).
[4] N.V. Nikonorov, V.M. Petrov. Optika i spektroskopiya **129**, *4*, 385 (2021). (in Russian).
[5] C. Thizy, Y. Stockman, P. Lemaire, Y. Houbrechts, A. Mazzoli, M. Georges, E. Mazy, I. Tychon, D. Doyle, G. Ulbrich. J. Photorefractiv. Effects, Mater. Dev. 707 (2005).
[6] M. Georges, O. Dupont, I. Zayer, Ph. Lemaire, T. Dewandre. J. Photorefractiv. Effects, Mater. Dev. 456 (2003).
[7] A.V. Il'insky. Dokt. dis., Dinamika fotoindutsirovannykh zaryadov i polej v vysokoomnykh kristallakh. L. (1992). 262 s. (in Russian).
[8] S.N. Mustafaeva, S.M. Asadov. Int. Workshop on Impedance Spectroscopy (IWIS). Chemnitz, Germany (2022). P. 102. doi: 10.1109/IWIS57888.2022.9975115.
[9] M.M. Abdullah. Kuwait J. Science **49**, *2*, 12 (2022).
[10] N.I. Sorokin, V.M. Kanevsky. FTT **65**, *9* 1538 (2023). (in Russian).
[11] P. Prem Kiran. Asian J. Physics **30**, *6*, 917 (2021).
[12] P. Petkova, P. Vasilev. J. Sci. Appl. Res. **5**, 146,(2014).
[13] M. Isik, S. Delice, H. Nasser, N.M. Gasanly, N.H. Darvishov, V.E. Bagiev. J. Mater. Sci. Semicond. Proc. **120**, 105286 (2020).
[14] P. Debaj. Izbrannye trudy. Stat'i 1909–1965. Nauka, L., (1987). 46 s. (in Russian).
[15] V.S. Vonsovsky, M.I. Katznel'son. Kvantovaya fizika tverdogo tela. Nauka, M. (1983). 391 s. (in Russian).
[16] P. Dirak. UFN **129**, *4*, 681 (1979). (in Russian).
[17] A.V. Il'inskij, E.B. Shadrin. FTT **66**, *5*, 708 (2024). (in Russian).
[18] F. Kremer, A. Schonhals, W. Broadband. Dielectric Spectroscopy. Springer-Verlag (2002). 118 p.
[19] Ammar Sarem, Talal Khalass. Tishreen Univer. J. Res. Sci. Studies. Basic Sci. Ser. **31**, *1*, 189 (2009).
[20] Y. Hu, D.C. Sinclair. Chem. Mater. **25**, 48 (2013).

Translated by I.Mazurov